



**Master's Program in Molecular Medicine  
at the Charité - Universitätsmedizin Berlin**



**Master's Thesis**

to earn the

**Master of Science in Molecular Medicine**

**Characterizing the Role of a GLUT1 Mutation in  
GLUT1-deficiency Syndrome**

Presented by

**Jingyuan Cheng**

Born on May 17th, 1993

First Evaluator: Professor Dr. Matthias Selbach

Second Evaluator: Professor Dr. Volker Haucke

Completed at AG Selbach, Max Delbrück Center for Molecular Medicine



# Abstract

Glucose transporter-1 (GLUT1) deficiency syndrome is a genetic disorder characterized by impaired glucose transport into the brain. One of the clinically identified pathogenic mutations is a Pro485-to-Leu substitution located in the cytoplasmic carboxyl tail of GLUT1, whose pathogenic mechanisms remain unclear. A previous *in vitro* proteomic screen from our group revealed that this GLUT1 mutation leads to specific interactions with clathrins, which is supported by the further bioinformatic finding that the mutation creates a novel dileucine motif known to mediate clathrin-dependent trafficking.

In this study we used stable inducible HEK293 cells to further investigate the effect of the GLUT1 mutation on the intracellular localization and trafficking of the protein. We showed that the wild-type GLUT1 mainly localizes to the plasma membrane, whereas the mutant GLUT1 mislocalizes to intracellular compartments and co-localizes with endocytosed transferrin, as well as early endosomal and late endosomal markers. Moreover, SILAC-based quantitative characterization of proximate proteins also identified increased proximate interaction of the mutant GLUT1 with proteins associated with endocytosis and endosomal compartments. Together, these data suggest that the GLUT1<sup>P485L</sup> mutation causes internalization of the GLUT1 protein via clathrin-mediated endocytosis, thus leading to GLUT1 deficiency syndrome.



# Contents

<b>Abstract</b>	<b>iii</b>
<b>1 Introduction</b>	<b>1</b>
1.1 The GLUT1 <sup>P485L</sup> mutation . . . . .	1
1.2 Clathrin-mediated endocytosis . . . . .	2
<b>2 Materials and methods</b>	<b>3</b>
<b>3 Results</b>	<b>11</b>
3.1 Assessment of GLUT1 inducible expression . . . . .	11
3.2 Proximity labeling of GLUT1 variants . . . . .	12
3.3 Co-localization study of GLUT1 variants . . . . .	12
<b>4 Discussion</b>	<b>13</b>
<b>Acknowledgements</b>	<b>17</b>
<b>Literature</b>	<b>19</b>



# List of Figures

2.1	Graphic map of the recombinant plasmids. . . . .	4
3.1	The doxycycline-inducible expression of GLUT1 variants. . . . .	11
3.2	The inducible expression and localization of GLUT1 variants. . . . .	12





## List of Tables

2.1	Primer sequences for GLUT1 cloning. . . . .	3
2.2	Antibodies used for Western blotting and their dilutions. . . . .	6
2.3	Antibodies for immunofluorescence and their dilutions. . . . .	9
2.4	Settings for fluorescence excitation and detection. . . . .	9



# Introduction

As the primary glucose transporter across the endothelial cells of the blood-brain barrier, the facilitated glucose transporter member 1 (GLUT1) protein plays a central role in the regulation of brain energy metabolism and maintenance of central nervous system homeostasis [1]. Human GLUT1 is encoded by the *SLC2A1* gene on the short arm of chromosome 1, consists of 492 amino acids and contains 12 transmembrane  $\alpha$  helices [2, 3]. GLUT1 is highly expressed in endothelial cells and glial cells, but is ubiquitously expressed at lower levels as well [4, 5]. Two isoforms of GLUT1 have been found, namely the 55kDa form with N-linked glycosylation at Asn45 and the 45kDa unglycosylated form [6, 7].

Mutations in the *SLC2A1* gene can result in GLUT1 deficiency syndrome (G1DS), an autosomal dominant disorder caused by impaired GLUT1-mediated glucose transport into the brain [8, 9]. To date, approximately 80 mutations in the *SLC2A1* gene have been detected in about 140 patients, including large-scale deletions, insertions, missense, nonsense, frame shift, translation initiation and splice-site mutations [10, 11]. These mutations are heterozygous resulting in GLUT1 haploinsufficiency - absence or loss of a functional allele [9, 11]. The classic G1DS phenotype consist of intractable epilepsy presenting in infancy, delayed neurologic development, secondary microcephaly and complex movement disorders [8, 9]. Milder variants have been reported to affect about 10% G1DS patients and present mental retardation, movement abnormalities but without clinical seizures [10, 12]. The diagnostic hallmark of G1DS features reduced cerebrospinal fluid (CSF) glucose concentration (hypoglycorrachia) combined with low CSF lactate and low 3-O-methyl-D-glucose uptake in erythrocytes [10, 13]. The ketonic diet, introduced as a treatment for G1DS in 1991, provides an alternative fuel for brain metabolism and effectively controls the seizures in G1DS patients [10].

## 1.1 The GLUT1<sup>P485L</sup> mutation

One of the clinically identified missense mutations in GLUT1 is a Pro485-to-Leu substitution (GLUT1<sup>P485L</sup>) located in the cytoplasmic carboxyl tail [1, 14]. However, the molecular

mechanisms by which the mutation causes the disease remains elusive. In a previous proteomic screen study to investigate the impact of disease-causing mutations, the GLUT1<sup>P485L</sup> mutation was found to lead to an increased binding of clathrins. Sequence analysis revealed that the mutation creates a dileucine motif known to mediate clathrin-dependent endocytosis ([D/E]XXXL[L/I]) in the cytoplasmic tail [15, 16].

## **1.2 Clathrin-mediated endocytosis**

Based on these findings, it is hypothesized that the GLUT1<sup>P485L</sup> mutation causes clathrin-mediated endocytosis and possibly subsequent degradation of GLUT1, leading to the development of GLUT1-deficiency syndrome. The hypothesis will be further investigated in this master thesis.

# Materials and methods

## Cell line generation

Stable HEK293 cell lines expressing the wild-type and mutant GLUT1 were kindly provided by Katrina Meyer and Markus Landthaler at Max Delbrück Center. In brief, the gene *SLC2A* was purchased from Harvard Plasmid Repository and a stop codon was added with the primers listed in Table 2.1. The P485L mutation was introduced by polymerase chain reaction-directed mutagenesis with the primers listed in Table 2.1. The wild-type and mutant *SLC2A* coding sequences were recombined into the vector pDEST-pcDNA5-BirA-FLAG N-term [17] using Gateway cloning system (ThermoFisher), as illustrated in Figure 2.1.

**Table 2.1: Primer sequences for GLUT1 cloning.**

Primer	Sequence from 5' to 3'
Stop codon forward	TCCCAAGTGTAATTGCCAACTTTCTTGTACAAAGTTG
Stop codon reverse	ATCAGCCCCCAGGGGATG
P485L forward	CTGTTCCATCtCCTGGGGGCT
P485L reverse	CTCCTCGGGTGTCTTGTCAC

For the generation of each cell line, 0.1 µg of the resulting vector was mixed with 0.9 µg pOG44 Flp-recombinase expression vector (ThermoFisher) and 2 µL Lipofectamine 200 (ThermoFisher) in 100 µL Opti-MEM (ThermoFisher). After incubation for 5 min, the transfection mixture was added to HEK293 Flp-In T-Rex cells. After growing for 48 hr, hygromycin (100 µg/mL, InvivoGen) was added and the cells were selected for 2-3 weeks by the addition of fresh hygromycin-containing cell culture media. A control HEK293 T-REx cell line was generated in a similar manner with an integrated transgene for the inducible expression of GFP1-10.

The three cell lines were stored in cryogenic vials (Croning) in liquid nitrogen. To recover cells, one vial of each cell line was removed from the liquid nitrogen tank and immediately warmed up to 37 °C. The contents were diluted in 10 mL pre-warmed DMEM (Life Technologies) complemented with 10% fetal bovine serum (Pan-Biotech). The medium is referred to as complete DMEM in the following. After spinning down at room temperature

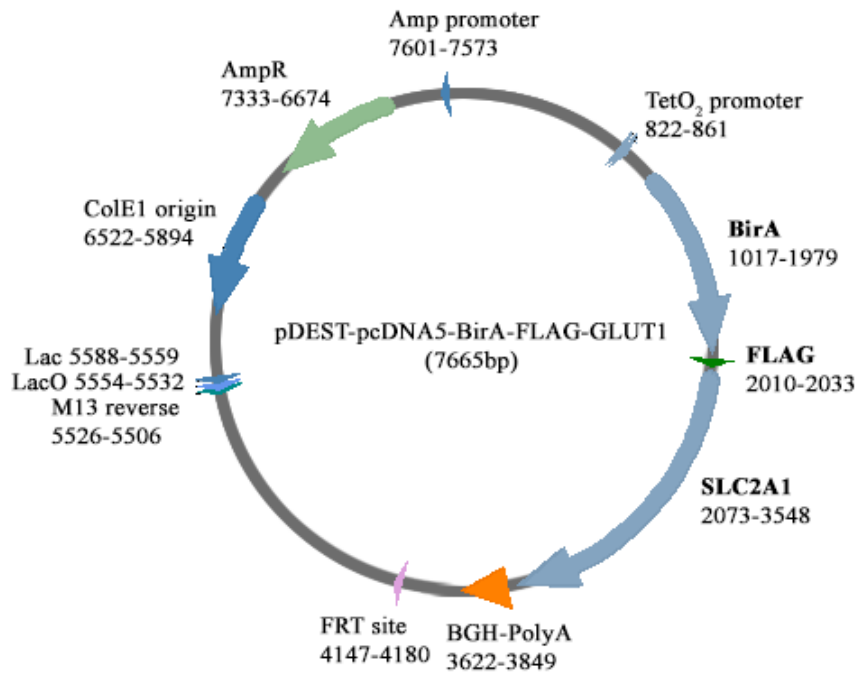


**Figure 2.1: Graphic map of the recombinant plasmids.**

and 500 rpm for 3 min, the cell pellets were resuspended in 10 mL complete DMEM and seeded in T-75 flasks (CELLSTAR).

### Cell culture

Stable HEK293 cells were cultured at 37 °C and 5% CO<sub>2</sub> in culture flasks at approximately 10% confluency in complete DMEM. Cells were routinely passaged twice a week as follows: the medium was aspirated and the cells were briefly washed with 4 mL sterile pre-warmed PBS (Life Technologies). To detach the cells 1 mL trypsin-EDTA (0.05%, Life Technologies) was added and the flask was placed in an incubator at 37 °C and 5% CO<sub>2</sub> for 1 min. Trypsin was then inactivated with 9 mL pre-warmed complete DMEM. The medium was gently pipetted to the bottom of the flask in order to recover all the cells and homogenize them. 1 mL of the cell suspension was transferred into 10 mL fresh complete DMEM in a new culture flask which was then placed back in the incubator. The cells would reach approximately 80% confluency before the next passaging.

Cells used for BioID experiments were cultured in SILAC DMEM (Life Technologies) complemented with glutamine (Glutamax, Life Technologies), pyruvate (Life Technologies), non-essential amino acids (Life Technologies) and 10% dialyzed fetal bovine serum (Pan-Biotech). In addition, L-arginine (Arg0, Sigma-Aldrich) and L-lysine (Lys0, Sigma-Aldrich)

were added to the Light SILAC DMEM to a final concentration of 0.199 mM and 0.339 mM, respectively. Alternatively, Arg6 and Lys4 or Arg10 and Lys8 were added in place of their Light counterparts to make Medium-heavy SILAC DMEM and Heavy SILAC DMEM, respectively. PBS-EDTA (Lonza) was used to detach the cells when passaging to avoid isotope contamination. After six passages cells were fully labeled as assessed by MS.

For the doxycycline induction experiments unlabeled HEK cells were cultured in 6-well plates. The cells were grown to approximately 50% confluency on the second day after seeding. The medium was removed and 2 mL complete DMEM containing doxycycline (Sigma-Aldrich) was carefully added to each well. After 24 hr or 48 hr the cells were harvested for Western blotting analysis.

For the BioID experiments fully labeled HEK293 cells were seeded in 15 cm plates with approximately 25% density. Two plates were used for each condition. HEK293 stable cells expressing GFP1-10 were labeled in Light SILAC DMEM and used as negative control cells. Besides the Light control cells, in the forward experiment mutant GLUT1 cells were cultured in Medium-heavy SILAC DMEM and wild-type GLUT1 cells were cultured in Heavy SILAC DMEM, while in the reverse label-swap experiment wild-type GLUT1 cells were cultured in Medium-heavy SILAC DMEM and mutant GLUT1 cells were cultured in Heavy SILAC DMEM. The cells were grown to 40%-50% confluency before being treated with 0.1 µg/mL doxycycline and 1 mM biotin (ThermoFisher). After 24 hr, the cells were scraped in ice-cold PBS and collected for further BioID purification and MS analysis.

For the immunofluorescence experiments sterile glass coverslips (Roth, 18 mm diameter, 0.170 mm thickness) were placed in 12-well plates. Poly-L-lysine (0.01%, Sigma-Aldrich) was added to each well to cover the coverslips. After incubation at room temperature for 5 min, poly-L-lysine was recovered from the wells and stored at 4 °C. The coverslips were washed twice with sterile H<sub>2</sub>O before being air-dried completely. HEK293 cells were then counted and seeded in the plate with approximately 25% density. The cells were treated with 0.1 µg/mL doxycycline on the second day and subjected to subsequent immunostaining on the third day.

### **Western blotting**

Cells were grown in 6-well plates as described above. After doxycycline or inhibitor treatment, cells were scraped in ice-cold PBS and spun down at 300 rcf, 4 °C for 4 min. Cell pellets were lysed for 15 min at room temperature in lysis buffer [50 mM ABC solution, 2% SDS, supplemented with 60 Units/mL benzonase (Sigma-Aldrich) and protease inhibitors (Roche)]. Lysates were spun down at 140 000 rpm for 15 min to remove cell debris and

supernatants were transferred to new Eppendorf tubes. For each SDS-PAGE sample, 15  $\mu$ L supernatant was diluted in LDS sample buffer (NOVEX) complemented with 1  $\mu$ L 1M DTT (Sigma-Aldrich) before being heated at 70 °C for 10 min in a thermoblock. Samples were then loaded onto a 4%-12% gel (NOVEX) along with protein ladders (PageRuler Plus, ThermoFisher). Proteins were separated using electrophoresis for 90 min at 150 V in 400 mL MES running buffer (ThermoFisher).

Before transferring a PVDF membrane (Merck Millipore) was activated in methanol for 1 min and equilibrated in ice-cold transfer buffer (25 mM Tris-HCl, 190 mM glycine, 20% methanol, pH 8.3) for 10 min. Whatman filter papers and sponges were also soaked in transfer buffer for 10 min. A tank blotting system (Invitrogen) was used to transfer the separated proteins to the membrane. In short, a transfer sandwich was prepared with the membrane on the cathode and the gel on the anode. Air bubbles between the gel and membrane were removed by rolling them out with a roller. The cassette was then placed in the transfer tank on ice and the proteins were transferred at a constant current of 250 mA for 2 hr.

After transferring the membrane was blocked in 5% milk powder in TBST (150 mM sodium chloride, 20 mM Tris-HCl, 0.1% Tween-20, pH 7.6) at room temperature for 30 min. The membrane was then incubated with the primary antibody diluted in blocking buffer while rotating at 4 °C. The membrane was washed 3 times for 5 min in TBST before being incubated at room temperature for 1 hr with the HRP-conjugated secondary antibody diluted in blocking buffer. The membrane was washed again before the chemiluminescence substrate (PerkinElmer) was applied to the membrane. The chemiluminescent signals were captured using a ChemiDoc MP Imaging System (Bio-Rad) and analyzed with Image Lab 5.2.1. The primary and secondary antibodies used in this thesis are summarized in Table 2.2.

**Table 2.2: Antibodies used for Western blotting and their dilutions.**

Antibodies	Source	Dilution	Conjugate
Rabbit polyclonal anti-FLAG	Cell Signaling Technology	1:1000	HRP
Rabbit polyclonal anti-LC3	Novus Biologicals	1:1000	
Mouse monoclonal anti- $\beta$ -actin	Sigma-Aldrich	1:10 000	
Anti-rabbit IgG	GE Healthcare	1:10 000	HRP
Anti-mouse IgG	GE Healthcare	1:25 000	HRP

## BioID and MS analysis



Cells scraped from 15 cm plates were spun down at 300 rcf at 4 °C for 4 min. After resuspension in ice-cold PBS, the triple SILAC labels were combined into a forward and a reverse experiment. The cells were spun down again and the cell pellets were resuspended in 1.5 mL of RIPA buffer (50 mM tris-HCl, 150 mM NaCl, 1% NP-40, 1 mM EDTA, 1 mM EGTA, 0.1% SDS, 1% sodium deoxycholate, pH 7.5, supplemented with 75 Units/mL benzonase and protease inhibitors). After incubation with agitation at 4 °C for 1 hr, the lysates were sonicated on ice for 3 min. The lysates were then centrifuged for 20 min at 16 100 rcf at 4 °C and the supernatants were transferred to 2 mL Eppendorf tubes.

For affinity purification a 180 µL bed volume of streptavidin T1 magnetic beads (Invitrogen) was washed in PBS twice and RIPA buffer once before being resuspended in 200 µL RIPA buffer. 100 µL of the bead solution was added to each lysate sample. Affinity purification was performed at 4 °C for 3 hr on a rotating wheel.

The beads were then carefully washed twice in RIPA buffer and twice in TAP lysis buffer (50 mM HEPES-KOH, 100 mM KCl, 10% glycerol, 2 mM EDTA, 0.1% NP-40, pH 8.0). The detergents were removed by washing three times in 50 mM ABC. The beads were resuspended in 200 µL ABC and 10 µL of 10 mM DTT in 50 mM ABC was added to reduce disulfide bonds of proteins. After 30 min incubation in a thermomixer at 30 °C at 500 rpm, 10 µL of 55 mM IAA (Sigma-Aldrich) in 50 mM ABC was added to alkylate the cysteine residues and the samples were incubated in the dark at 30 °C at 500 rpm for 30 min. The samples then were digested with 1.5 µg trypsin (Promega) and incubated overnight at 30 °C at 1100 rpm. On the next day, the tryptic peptides were separated from beads with a magnetic rack and transferred to fresh 1.5 mL tubes. The digestion was stopped by adding 10 µL 10% TFA and the tryptic peptides were loaded on C18 StageTip columns for purification. After washing with sample buffer (3% TFA, 5% acetonitrile) twice, the peptides were eluted from the columns into an autosampler plate with 50 µL buffer B (0.1% formic acid, 80% acetonitrile). A vacuum centrifuge (Eppendorf) was used to evaporate the solvent and 8 µL buffer A (5% acetonitrile, 0.1% formic acid) was added to the samples.

Peptides were separated on a reverse-phase column on a High Performance Liquid Chromatography (HPLC) system (ThermoScientific) with a gradient set up as the following ratios of buffer B in buffer A: 2 min at 250 µL/min with a linear gradient from 5% to 6% buffer B, 18 min at 200 µL/min from 6% to 8%, 80 min at 200 µL/min from 8% to 20%, 80 min at 200 µL/min from 20% to 33%, 20 min at 200 µL/min from 33% to 45%, 2 min at 200 µL/min from 45% to 60%, 1 min at 250 µL/min from 60% to 95%, 5 min at 250 µL/min with 95% buffer B, 1 min at 250 µL/min from 95% to 75%, and 5 min at 250 µL/min at 75% buffer B. Peptides were ionized using an electrospray ionization source (ThermoScientific)

and analyzed on a Q-Exactive Plus Orbitrap instrument (ThermoScientific). The mass spectrometer was operated with Xcalibur in data-dependent acquisition mode with the following parameters: a full MS scan (resolution: 70 000, scan range: 300 to 1700 m/z, AGC target: 1 000 000 ions, maximum injection time: 120 ms) followed by MS-MS analysis (resolution: 17 500, AGC target: 100 000 ions, maximum injection time: 60 ms) on the top 10 abundant ions.

The resulting raw files were analyzed using MaxQuant 1.5.2.8 [18]. The reference human proteome database, consisting of 159 616 entries, was downloaded from the UniProt Knowledgebase on February 28th, 2017. Lys4, Arg6 and Lys8, Arg10 were added to the labels. Variable modifications were set as N-terminal acetylation and oxidation of methionines. The *in silico* digestion of peptides in the reference database was performed with trypsin/P site-specific cleavage. Default global parameters were kept except that "re-quantify" and "match between runs" were turned on. The false discovery rate, assessed by in-parallel searching in a decoy database generated by reversing the reference database, was set to 0.01 at peptide and protein levels. The following analysis and graphics were performed using Perseus and R 3.3.3.

### **Transferrin uptake**

After 24 hr of doxycycline induction, the cells were starved for 1 hr in serum-free medium supplemented with 20 mM HEPES (Life Technologies). Transferrin conjugated with Alexa Fluor 568 (Life Technologies) was diluted in starvation buffer to a final concentration of 10 µg/mL and droplets of 35 µL transferrin solution were pipetted onto a parafilm in a dark humid chamber. The coverslips were then carefully lifted off the bottom of the plate with forceps and placed face-down on the droplets. The humid chamber was incubated at 37 °C and 5% CO<sub>2</sub> for 10 min. After transferrin uptake, the coverslips were washed 3 times for 5 min with PBS supplemented with 10 mM MgCl<sub>2</sub> and 10 mM CaCl<sub>2</sub>, followed by standard immunostaining procedures described as below.

### **Immunostaining and confocal microscopy**

Prior to staining, cell culture medium was aspirated and cells were briefly washed with pre-warmed PBS. The cells were fixed in 4% PFA for 15 min at room temperature before being washed 3 times for 5 min in PBS. To permeabilize cells and block unspecific binding sites the cells were incubated for 1 hr at room temperature in blocking buffer [5% goat serum (Sigma-Aldrich), 0.3% Triton X-100 (Sigma-Aldrich) in PBS]. The primary antibody was

diluted in antibody dilution buffer [1% BSA - Fraction V (Sigma-Aldrich), 0.3% Triton X-100 in PBS], as indicated in Table 2.3. The coverslips were placed face-down on droplets of 50  $\mu$ L primary antibody solution on a piece of parafilm in a dark humid chamber. After 1 hr incubation at room temperature, the coverslips were placed face-up in the plate and washed 3 times for 5 min in PBS. Similarly, the coverslips were incubated with secondary antibody solution for 1 hr at room temperature in the humid chamber before being washed for 5 min in PBS. The coverslips were then counterstained with DAPI (0.1  $\mu$ g/mL in PBS, Sigma-Aldrich) for 3 min and washed for 10 min in PBS. Finally, the coverslips were rinsed briefly in MilliQ H<sub>2</sub>O and mounted with ProLong Gold Antifade Mountant (Life Technologies) on slides. After overnight incubation, the slides were stored at 4 °C in the dark.

**Table 2.3: Antibodies for immunofluorescence and their dilutions.**

Antibodies	Source	Dilution	Conjugate
Mouse monoclonal anti-FLAG	Sigma-Aldrich	1:200	
Rabbit monoclonal anti-EEA1	Cell Signaling Technology	1:100	
Rabbit monoclonal anti-Rab4	Cell Signaling Technology	1:100	
Rabbit monoclonal anti-Rab9	Cell Signaling Technology	1:100	
Rabbit monoclonal anti-Rab11	Cell Signaling Technology	1:100	
Rabbit monoclonal anti-LAMP1	Cell Signaling Technology	1:100	
Goat anti-Mouse IgG (H+L)	Invitrogen	1:500	Alexa Fluor 488
Donkey anti-Rabbit IgG (H+L)	Invitrogen	1:500	Alexa Fluor 568

Images in this thesis were acquired using Leica DMI6600 confocal laser scanning microscope with an HCX PL APO 63.0 $\times$ /1.40 oil objective. As summarized in Table 2.4, fluorophores were excited using 405 nm laser diode, Argon 488 nm laser (20% power) or DPSS 561 nm laser and detected using photomultiplier tubes (PMT). The pinhole diameter was set to 95.6  $\mu$ m, scanning mode was unidirectional, line average was 2, sampling speed was 400 Hz. For co-localization studies the zoom was set to 5 and the voxel size was 48.1 nm (width)  $\times$  48.1 nm (height)  $\times$  125.9 nm (depth).

**Table 2.4: Settings for fluorescence excitation and detection.**

Fluorophore	Laser line	Laser intensity	PMT	PMT gain	PMT offset
DAPI	405 nm	8.00%	413-477 nm	619 V	-1
Alexa 488	488 nm	12.00%	506-598 nm	646 V	-1
Alexa 568	561 nm	15.00%	580-710 nm	619 V	-1

The z-stack confocal microscopy images were further analyzed using ImageJ 1.51j. The stack viewing and color options were set as the default configuration of the Bio-Formats

plugin. One z slice was selected in each image to represent all stacks. The brightness and contrast of the channels were uniformly adjusted in each staining experiment and a 10  $\mu\text{m}$  scale bar was added to the images.

# Results

## 3.1 Assessment of GLUT1 inducible expression

Previous results from the work of our laboratory showed that the GLUT1<sup>P485L</sup> mutation leads to specific interaction with clathrins and internalization of the protein. In order to further investigate the role and functional effects of the mutation, we generated two Flp-In T-Rex HEK293 cell lines containing inducible BirA-FLAG epitope-tagged full length wild-type or mutant GLUT1 (Figure 2.1).

To determine the optimal conditions for inducible expression, GLUT1 wild-type and mutant cells were grown in different concentrations of doxycycline for 24 hr and the expression of the GLUT1 protein was analyzed by Western blotting. The results showed that (Figure 3.1 A).

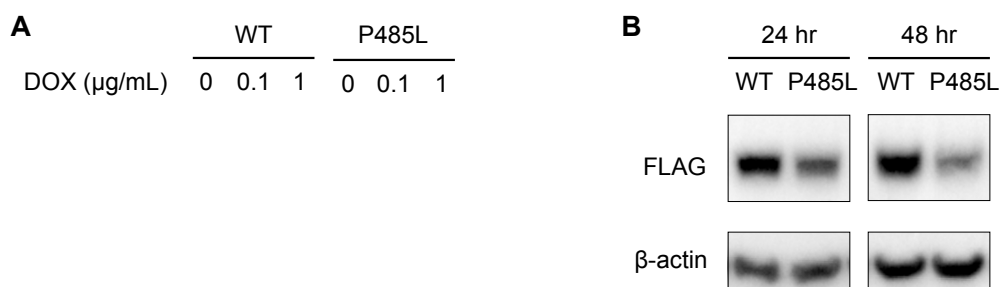


**Figure 3.1: The doxycycline-inducible expression of GLUT1 variants.**

GLUT1 wild-type and mutant cells

Two different induction times were tested

In addition, the doxycycline-inducible expression of GLUT1 was confirmed by confocal immunofluorescence microscopy. GLUT1 wild-type and mutant cells were grown on coverslips and incubated in medium with or without doxycycline for 24 hr. Immunostaining was performed with monoclonal mouse anti-FLAG and Alexa 488-conjugated anti-mouse antibodies. A low level of GLUT1 expression was observed in a small fraction of uninduced wild-type cells (Figure 3.2 A).

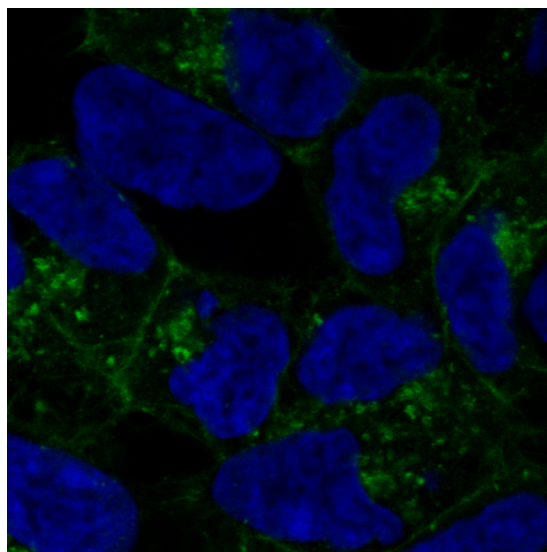


**Figure 3.2: The inducible expression and localization of GLUT1 variants.**

GLUT1 wild-type and mutant cells were cultured for 24 hr either in the absence or presence of 0.1  $\mu\text{g/mL}$  doxycycline. The expression of GLUT1 was assessed by immunofluorescence microscopy. A small subpopulation of uninduced wild-type cells showed weak expression of GLUT1 (A)

### **3.2 Proximity labeling of GLUT1 variants**

### **3.3 Co-localization study of GLUT1 variants**

## **Discussion**





# List of Abbreviations

<b>ABC</b>	Ammonium bicarbonate
<b>AGC</b>	Automatic gain control
<b>BSA</b>	Bovine serum albumin
<b>CPZ</b>	Chlorpromazine
<b>CSF</b>	Cerebrospinal fluid
<b>DAPI</b>	4',6-Diamidino-2-phenylindole
<b>DMEM</b>	Dulbecco's modified Eagle's medium
<b>DOX</b>	Doxycycline
<b>DPSS</b>	Diode-pumped solid-state
<b>DTT</b>	Dithiothreitol
<b>EDTA</b>	Ethylenediaminetetraacetic acid
<b>GFP</b>	Green fluorescent protein
<b>GLUT1</b>	Facilitated glucose transporter member 1
<b>G1DS</b>	Glucose transporter 1 deficiency syndrome
<b>HEK</b>	Human embryonic kidney
<b>HEPES</b>	4-(2-Hydroxyethyl)-1-piperazineethanesulfonic acid)
<b>HPLC</b>	High-pressure liquid chromatography
<b>HRP</b>	Horseradish peroxidase
<b>IAA</b>	Iodoacetamide
<b>MS</b>	Mass spectrometry
<b>MS/MS</b>	Tandem mass spectrometry
<b>PBS</b>	Phosphate-buffered saline
<b>PFA</b>	Paraformaldehyde
<b>PMT</b>	Photomultiplier tube
<b>PVDF</b>	Polyvinylidene fluoride
<b>rcf</b>	Relative centrifugal force
<b>RIPA</b>	Radioimmunoprecipitation assay
<b>rpm</b>	Revolutions per minute

<b>SDS-PAGE</b>	Sodium dodecyl sulfate polyacrylamide gel electrophoresis
<b>SILAC</b>	Stable isotope labeling by amino acids in cell culture
<b>TAP</b>	Tandem affinity purification
<b>TBST</b>	Tris buffered saline with tween 20
<b>TFA</b>	Trifluoroacetic acid
<b>TGN</b>	Trans-Golgi network
<b>Tris</b>	Tris(hydroxymethyl)aminomethane
<b>WT</b>	Wild-type

## Acknowledgements

This study was carried out in the Protein Dynamics Laboratory at Max Delbrück Center of Molecular Medicine. I would like to thank Professor Matthias Selbach for having given me the opportunity to complete my Master's thesis in his laboratory. I am also very grateful to my thesis supervisor Katrina Meyer who introduced me to this extraordinarily interesting project and offered me continuous support throughout the thesis. Her guidance and encouragement has been most inspiring and education.



## References

- [1] J. M. Pascual, D. Wang, R. Yang, L. Shi, H. Yang, and D. C. De Vivo, “Structural signatures and membrane helix 4 in glut1: inferences from human blood-brain glucose transport mutants,” *The Journal of Biological Chemistry* **283**, 16732–16742 (2008).
- [2] M. Mueckler, “Facilitative glucose transporters,” *European Journal of Biochemistry* **219**, 713–725 (1994).
- [3] M. Uldry and B. Thorens, “The slc2 family of facilitated hexose and polyol transporters,” *Pflügers Archiv* **447**, 480–489 (2004).
- [4] W. L. Lee and A. Klip, “Shuttling glucose across brain microvessels, with a little help from glut1 and amp kinase. focus on ‘amp kinase regulation of sugar transport in brain capillary endothelial cells during acute metabolic stress’,” *American Journal of Physiology - Cell Physiology* **303**, C803–C805 (2012).
- [5] T. J. Wheeler and P. C. Hinkle, “The glucose transporter of mammalian cells,” *Annual Review of Physiology* **47**, 503–517 (1985).
- [6] M. M. M. Paul W. Hruz, “Structural analysis of the glut1 facilitative glucose transporter,” *Molecular Membrane Biology* **18**, 183–193 (2001).
- [7] R. Duelli and W. Kuschinsky, “Brain glucose transporters: relationship to local energy demand,” *Physiology* **16**, 71 (2001).
- [8] D. C. De Vivo, R. R. Trifiletti, R. I. Jacobson, G. M. Ronen, R. A. Behmand, and S. I. Harik, “Defective glucose transport across the blood-brain barrier as a cause of persistent hypoglycorrhachia, seizures, and developmental delay,” *New England Journal of Medicine* **325**, 703–709 (1991).
- [9] J. Klepper, M. Willemsen, A. Verrips, E. Guertsen, R. Herrmann, C. Kutzick, A. Flörcken, and T. Voit, “Autosomal dominant transmission of glut1 deficiency,” *Human Molecular Genetics* **10**, 63–68 (2001).
- [10] D. Wang, J. M. Pascual, H. Yang, K. Engelstad, S. Jhung, R. P. Sun, and D. C. De Vivo, “Glut-1 deficiency syndrome: clinical, genetic, and therapeutic aspects.” *Annals of Neurology* **57**, 111–118 (2005).

- 
- [11] W. G. Leen, J. Klepper, M. M. Verbeek, M. Leferink, T. Hofste, B. G. van Engelen, R. A. Wevers, T. Arthur, N. Bahi-Buisson, D. Ballhausen, J. Bekhof, P. van Bogaert, I. Carrilho, B. Chabrol, M. P. Champion, J. Coldwell, P. Clayton, E. Donner, A. Evangeliou, F. Ebinger, K. Farrell, R. J. Forsyth, C. G. E. L. de Goede, S. Gross, S. Grunewald, H. Holthausen, S. Jayawant, K. Lachlan, V. Laugel, K. Leppig, M. J. Lim, G. Mancini, A. D. Marina, L. Martorell, J. McMenamin, M. E. C. Meuwissen, H. Mundy, N. O. Nilsson, A. Panzer, B. T. Poll-The, C. Rauscher, C. M. R. Rouselle, I. Sandvig, T. Scheffner, E. Sheridan, N. Simpson, P. Sykora, R. Tomlinson, J. Trounce, D. Webb, B. Weschke, H. Scheffer, and M. A. Willemsen, “Glucose transporter-1 deficiency syndrome: the expanding clinical and genetic spectrum of a treatable disorder,” *Brain* **133**, 655–670 (2010).
- [12] A. Suls, P. Dedeken, K. Goffin, H. Van Esch, P. Dupont, D. Cassiman, J. Kempfle, T. V. Wuttke, Y. Weber, H. Lerche, Z. Afawi, W. Vandenberghe, A. D. Korczyn, S. F. Berkovic, D. Ekstein, S. Kivity, P. Ryvlin, L. R. F. Claes, L. Deprez, S. Maljevic, A. Vargas, T. Van Dyck, D. Goossens, J. Del-Favero, K. Van Laere, P. De Jonghe, and W. Van Paesschen, “Paroxysmal exercise-induced dyskinesia and epilepsy is due to mutations in *slc2a1*, encoding the glucose transporter *glut1*,” *Brain* **131**, 1831–1844 (2008).
- [13] J. Klepper and B. Leiendecker, “Glut1 deficiency syndrome–2007 update,” *Developmental Medicine and Child Neurology* **49**, 707–716 (2007).
- [14] L. Slaughter, G. Vartzelis, and T. Arthur, “New *glut-1* mutation in a child with treatment-resistant epilepsy,” *Epilepsy Research* **84**, 254–256 (2009).
- [15] K. N. Pandey, “Functional roles of short sequence motifs in the endocytosis of membrane receptors,” *Frontiers in Bioscience (Landmark Ed)* **14**, 5339–5360 (2009).
- [16] H. Dinkel, K. Van Roey, S. Michael, M. Kumar, B. Uyar, B. Altenberg, V. Milchevskaya, M. Schneider, H. Kühn, A. Behrendt, S. L. Dahl, V. Damerell, S. Diebel, S. Kalman, S. Klein, A. C. Knudsen, C. Mäder, S. Merrill, A. Staudt, V. Thiel, L. Welti, N. E. Davey, F. Diella, and T. J. Gibson, “Elm 2016—data update and new functionality of the eukaryotic linear motif resource,” *Nucleic Acids Research* **44**, D294–D300 (2016).
- [17] A. L. Couzens, J. D. R. Knight, M. J. Kean, G. Teo, A. Weiss, W. H. Dunham, Z.-Y. Lin, R. D. Bagshaw, F. Sicheri, T. Pawson, J. L. Wrana, H. Choi, and A.-C. Gingras,

- “Protein interaction network of the mammalian hippo pathway reveals mechanisms of kinase-phosphatase interactions,” *Science Signaling* **6**, rs15 (2013).
- [18] J. Cox, M. Y. Hein, C. A. Lubner, I. Paron, N. Nagaraj, and M. Mann, “Accurate proteome-wide label-free quantification by delayed normalization and maximal peptide ratio extraction, termed MaxLFQ,” *Molecular & Cellular Proteomics : MCP* **13**, 2513–2526 (2014).